Incorporating Fuzziness in Spatial Susceptible-Infected Epidemic Models

Jan M. Baetens Bernard De Baets

KERMIT, Department of Applied Mathematics, Biometrics and Process Control
Ghent University, Coupure Links 653, 9000 Gent, Belgium
Email: jan.baetens@ugent.be, bernard.debaets@ugent.be

Abstract— *In this paper we propose a coupled-map lattice for modelling epidemic spread in a fuzzy setting. The presented model complies with the need for adequate modelling tools to describe and/or predict spatio-temporal phenomena, following the growing availability of spatio-temporal data. Furthermore, our approach does not rely on partial differential equations making it particularly suited to model epidemics in a fuzzy setting. It will be shown that the presented model allows to describe epidemic spread when the magnitude of the initial outbreak and/or the epidemic properties are only imprecisely known.*

Keywords— epidemic, discrete model, fuzzy initial condition, spatio-temporal dynamics

1 Introduction

Ordinary differential equations (ODEs) are widely used and well established to model various biological phenomena, as illustrated extensively in [1]. Partial differential equations (PDEs) are often resorted to if one is not merely interested in the process' temporal dynamics but also in the spatial patterns it generates [2]. Recently, several researchers have addressed the (numerical) solution of fuzzy ODEs (FODEs) [3, 4], endorsed by their potential importance in various scientific fields, for including imprecise information into well-established mathematical models (see [3, 5]). At present, the study of FODEs is still growing [6, 7], while thorough research on fuzzy PDEs is not yet carried out. Two distinct approaches have been developed within the theory of FODEs, differing only in whether they rely upon the notion of fuzzy derivatives or not [8]. This dichotomy and the immaturity of the theory of FODEs and FPDEs might hamper the widespread consideration of fuzziness within mathematical biology, despite often being faced with imprecise information. To overcome these barriers, we propose a coupled-map lattice (CML), developed by [9], to work with fuzzy initial conditions and/or parameters easily in a spatially explicit context. A short overview of fuzziness in discrete dynamical systems will be presented in the first section of this paper. In the second section we will introduce the CML which will be used to model spatio-temporal epidemic dynamics. In the third section we will deal with fuzzy initial conditions, while fuzzy parameters will be treated in the last section.

2 Fuzziness in discrete dynamical systems

A cellular automaton (CA), first introduced by von Neumann and Ulam as 'cellular spaces', and explored in detail by Wolfram [10, 11], is a mathematical model, discrete in all its senses, e.g. space is represented by an infinite lattice of cells, updates occur only at discrete time steps and the states can only take a finite number of values [10]. CA and CML are closely related, but in the latter states can take arbitrary values [12]. Although the first notion of a fuzzy CA dates back to the late 60s [13], literature on fuzzy CA is considered insufficient [14]. Fuzzy automata were first defined by Wee and Fu [13], but several alternative definitions have been proposed [14, 15]. Essentially, every state is attributed a membership value in a fuzzy CA [15], as such relaxing the condition of merely allowing discrete states. Recently, a review on fuzzy automata has been published [14], following the increasing number of articles published on the topic (see [16, 17, 18]). Despite the definition given in [13], fuzzy CA are often simply understood as spatial extensions of fuzzy rule-based models such as Mamdami-Assilian [19, 20] or Takagi-Sugeno models [21], e.g. CA in which the local transition function is a fuzzy rule-based model (see [22, 23, 24, 25, 26, 27]). To our knowledge, the notion of fuzziness in CML models has not been addressed yet.

3 Spatially explicit modelling of epidemics

3.1 The model

Several authors, including Kaneko [12] and Wolfram [11], have argued that CML and CA provide a suitable framework to deal with spatio-temporal dynamics. This is illustrated by the rich variety of such models that has been developed during the last decade for describing various spatial biological phenomena such as epidemics [28, 29, 30], population dynamics [31, 32], tumor growth [33, 34, 35], biofilm development [36, 37] and much other phenomena [38, 39].

Recently, Baetens and De Baets [9] proposed a generalized CML for modelling various biological phenomena, traditionally described by means of PDEs. Their model is general in two senses. Firstly, exploiting graph notations makes it independent from the spatial subdivisions used to discretize the space domain and secondly, it can serve as a basis for modelling various biological phenomena. With regard to an epidemic sweeping through a region which is subdivided into irregular polygons, and involving only non-reproducing susceptible and infected individuals, it can be written in a simplified form as

$$\begin{cases} S_j^{t+1} = S_j^t - S_j^t \displaystyle\sum_{P_k \in N(P_j)} w_{jk}\, G\left(\mathbf{I}_j, d_{jk}\right)\, I_k^t \\ I_j^{t+1} = I_j^t + S_j^t \displaystyle\sum_{P_k \in N(P_j)} w_{jk}\, G\left(\mathbf{I}_j, d_{jk}\right)\, I_k^t \end{cases} \tag{1}$$

where S_j^t, resp. I_j^t, represent the fraction of susceptible, resp. infected individuals within polygon P_j at the t-th time step

ISBN: 978-989-95079-6-8

and G is a function describing the effect of landscape and connectivity characteristics on the epidemic spread, d_{jk} is the distance measured on a graph between the vertices v_j and v_k, representing polygons P_j and P_k, $N(P_j)$ is the set of polygons of which the infected inhabitants can affect I_j^{t+1}, e.g. the neighbourhood of P_j defined as

$$N(P_j) = \{P_k \in P \mid d_{ij} \leq \epsilon\} \,, \tag{2}$$

where ϵ is the neighbourhood radius. Further, w_{jk} is a weighting factor, weighing the influence of every $P_k \in N(P_j)$ in the determination of S_j^{t+1}, and $\mathbf{I}_j$ contains information about P_j. This model may be regarded as a discrete analogue of the PDE-based SI-model (see [2]). Assuming $S_j^t + I_j^t = 1$, at all t, and for all P_j, we only have to keep track of one of the system's equations in order to follow its dynamics. From (1) it follows clearly that the system has a single fixed point $\left(S_j^*, I_j^*\right) = (0, 1)$.

Within the framework of this paper, only a rectangular lattice consisting of 101×101 equally-sized cells will be considered, since we rather want to focus on the fuzziness in (1) than on its general applicability as discussed in [9]. Moreover, we will assume that the region is spatially homogeneous, e.g. G does not depend on $\mathbf{I}_j$, reducing (1) to

$$I_j^{t+1} = I_j^t + S_j^t \sum_{P_k \in N(P_j)} w_{jk}\, H\left(d_{jk}\right)\, I_k^t \,, \tag{3}$$

where we introduced the function H, only dependent on d_{jk}, to distinguish from G, potentially dependent on both d_{jk} and $\mathbf{I}_j$. Further, we will define

$$H\left(d_{jk}\right) = \begin{cases} \nu_0, \text{ if } d_{jk} = 0, \\ \nu_1, \text{ if } d_{jk} = 1, \\ \quad \vdots \\ \nu_\epsilon, \text{ if } d_{jk} = \epsilon, \end{cases} \tag{4}$$

where ϵ is the neighbourhood radius and ν_ϵ is a measure for the epidemic's virulence, in such a way that

$$\sum_{P_k \in N(P_j)} w_{jk}\, H\left(d_{jk}\right) \leq 1, \quad \forall\, t,\, P_j \,, \tag{5}$$

assuring that $0 \leq I_j^t \leq 1$, at all t, and for all P_j. For this paper, let $\epsilon = 1$, $w_{jk} = \frac{1}{8}$ for all j, k and $j \neq k$ and $w_{jk} = 1$ if $j = k$. Consequently, P_j's eight nearest neighbours influence I_j^{t+1} to the same degree.

3.2 Fuzziness in the proposed model

In the remainder of this paper S_j^t and I_j^t are considered fuzzy intervals in $[0, 1]$, while the notations $\left[S_j^t\right]^\alpha$ and $\left[I_j^t\right]^\alpha$ will refer to their respective α-cuts defined by $\left[S_j^t\right]^\alpha = \left\{s \in [0,1] \mid S_j^t(s) \geq \alpha\right\}$ if $\alpha > 0$ and $\left[S_j^t\right]^0 = \text{cl}\left\{s \in [0,1] \mid S_j^t(s) > 0\right\}$ (the closure of the support) if $\alpha = 0$, and analogously for $\left[I_j^t\right]^\alpha$. In consequence, we can write $\left[S_j^t\right]^\alpha = \left[s_{j,1}^t(\alpha), s_{j,2}^t(\alpha)\right]$ and $\left[I_j^t\right]^\alpha = \left[i_{j,1}^t(\alpha), i_{j,2}^t(\alpha)\right]$. A triangular fuzzy interval A will be denoted as $A \equiv (l, u, r)$ where $[A]^0 = [l, r]$ and $[A]^1 = \{u\}$. Two sources of fuzziness in (3) will be examined more closely. A first concerns the initial conditions I_k^0 necessary to iteratively solve (3). As indicated by Beale [40], spatial epidemiological data are becoming increasingly available, providing the means to deduce I_k^0. Nonetheless, one has to be aware of the imprecision in the outbreak data which can be modeled with a fuzzy set approach. Analogously, the parameters in (4) might only be known imprecisely, and will be regarded as the second source of fuzziness. Since the mathematical functions in (3) are restricted to the basic arithmetic operations and involve no derivatives, it becomes relatively straightforward to obtain the fuzzy system's spatio-temporal dynamics. Nonetheless, one has to bear in mind the coupling between S_j^t and I_j^t through the condition $S_j^t + I_j^t = 1$, at all t, and for all P_j. As such, S_j^t and I_j^t cannot take values independently of each other and may be called interactive fuzzy variables [41]. Their joint possibility distribution C_j^t is not given by $S_j^t \times I_j^t$ as illustrated in Fig. 1(a), but can be defined as [42]

$$\left[C_j^t\right]^\alpha = \left\{l\left(s_{j,1}^t(\alpha), i_{j,2}^t(\alpha)\right) + (1-l)\left(s_{j,2}^t(\alpha), i_{j,1}^t(\alpha)\right) \mid l \in [0,1]\right\} \,, \tag{6}$$

for all $\alpha \in [0, 1]$, and is depicted in Fig. 1(b). The extension $f(S_j^t, I_j^t)$ is defined by [43]

$$f(S_j^t, I_j^t)\,(z) = \sup_{f(x,y)=z} C_j^t\,(x, y) \,. \tag{7}$$

Following the theory outlined in [44], S_j^t and I_j^t may be called completely negatively 'correlated'. In view of the existing interactivity we can write

$$\left[S_j^t + I_j^t\right]^\alpha = \left[s_{j,1}^t(\alpha) + i_{j,2}^t(\alpha), s_{j,2}^t(\alpha) + i_{j,1}^t(\alpha)\right] \,, \tag{8}$$

and

$$\left[S_j^t \cdot I_j^t\right]^\alpha = \left[\min\left(s_{j,2}^t(\alpha) \cdot i_{j,1}^t(\alpha), s_{j,1}^t(\alpha) \cdot i_{j,2}^t(\alpha)\right), \max\left(s_{j,2}^t(\alpha) \cdot i_{j,1}^t(\alpha), s_{j,1}^t(\alpha) \cdot i_{j,2}^t(\alpha)\right)\right] \,. \tag{9}$$

All simulations were performed in Mathematica 6.0 (Wolfram Research, Inc.) on a desktop PC with an Intel Dual Core 1.86 GHz processor. Although a quadratic lattice was used in this paper, the described simulations can easily be performed when irregular spatial subdivisions would be utilized.

4 Fuzzy initial conditions

In this section, we assume $\nu_0 = 0.5$ and $\nu_1 = 0.5$, meaning that the spread of an infection in a polygon P_j can be equally attributed to infected individuals living in P_j as to infected individuals residing in P_j's neighbourhood. First, we will consider the situation in which a disease outbreak was recorded in the center polygon P_c of the grid, but only imprecise information was available on the proportion of initially infected individuals. As such, we adopted the following initial condition

$$\begin{cases} I_j^0 = (0.2, 0.3, 0.4) \,, \text{ if } j = c \\ I_j^0 = 0 \qquad\qquad\quad \,, \text{ else.} \end{cases} \tag{10}$$

Figure 2 illustrates the CML evolution during the first time interval: starting from the initial condition (Fig. 2(a), 2(d)),

ISBN: 978-989-95079-6-8

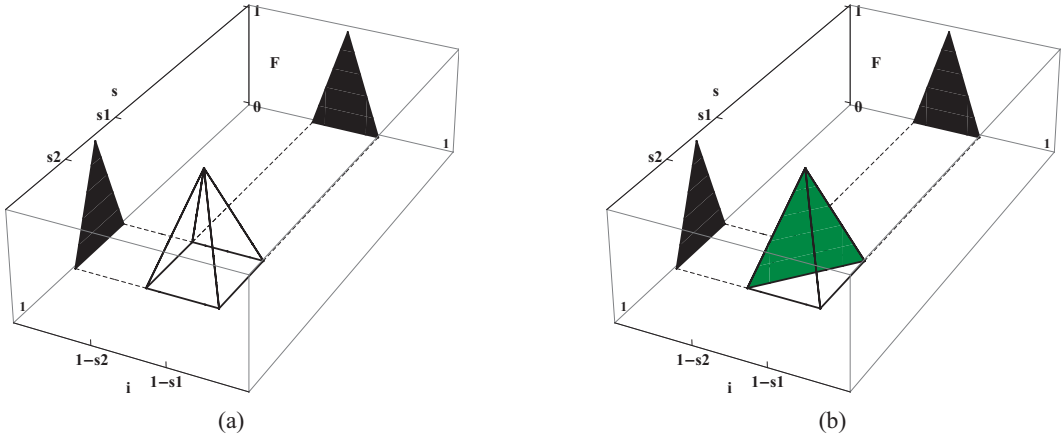

Figure 1: Non-interactive (a) and interactive (b) joint possibility distributions.

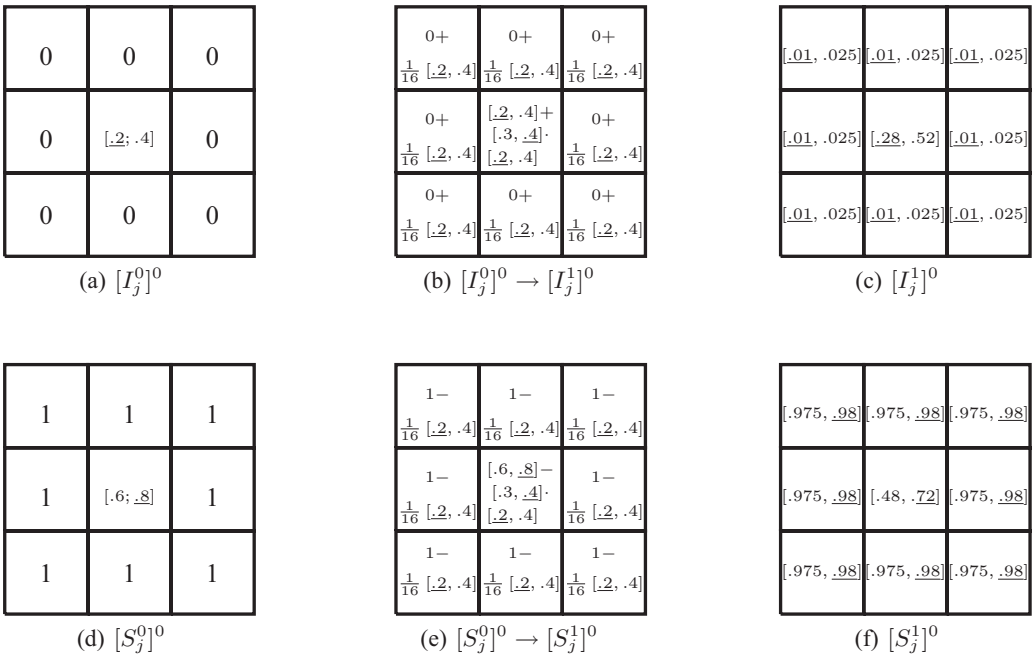

Figure 2: Evolution from $\left[I_j^0\right]^0$ to $\left[I_j^1\right]^0$ (a, b, c) and from $\left[S_j^0\right]^0$ to $\left[S_j^1\right]^0$ (e, d, f).

the lattice sites are updated according to (3), yielding the updated fuzzy states (Fig. 2(c), 2(f)). Since the neighbourhood was restricted to the nearest neighbours, it suffices to plot only the center polygon and its nearest neighbours to view all state changes during the first time interval. Underlining was used in order to visualize how the interaction between S_j^t and I_j^t was taken into account. For instance, $\left[I_j^1\right]^0$ was calculated as

$$\begin{aligned}\left[I_j^1\right]^0 &= \left[I_j^0\right]^0 + \left[s_{j,2}^0(0)\cdot\tfrac{1}{2}\,i_{j,1}^0(0),\; s_{j,1}^0(0)\cdot\tfrac{1}{2}\,i_{j,2}^0(0)\right]\\ &= [0.2, 0.4] + [0.8\cdot 0.1, 0.6\cdot 0.2]\\ &= [0.28, 0.52]\end{aligned}$$

Figure 3 shows the proportion of infected individuals after two, five, ten and fifteen time steps following the epidemic outbreak. For reasons of clarity, we limited the depicted spatial extent. The fill color of the polygons corresponds to the value of $\left[I_j^t\right]^1$, while the vertical axis indicates the membership value of all $i \in [0, 1]$. For each polygon, the fuzzy interval $I_j^t(i)$ is depicted at the center of the Y-direction, with the i-values marked along the X-direction, as indicated by the additional axis drawn at the back of the plots depicted in Fig. 3(a). This figure shows clearly that, although the epidemic was caused by an imprecise number of infected individuals residing in the center polygon, I_c^5's support was narrower than that of I_c^0, meaning that the imprecision of the model prediction decreased in this polygon during the considered time interval. This suggests that I_j^t tended to a crisp number as $t \rightarrow \infty$ which was verified experimentally by running the model for 150 time steps. This tendency could be expected since $(S_c^*, I_c^*) = (0, 1)$ is an asymptotic fixed point of the CML. Further, it is shown in this figure that the imprecision, initially only present in the outbreak data from the center polygon, propagated radially as a traveling wavefront giving rise to fuzziness in the model predictions at other locations. Though,

ISBN: 978-989-95079-6-8

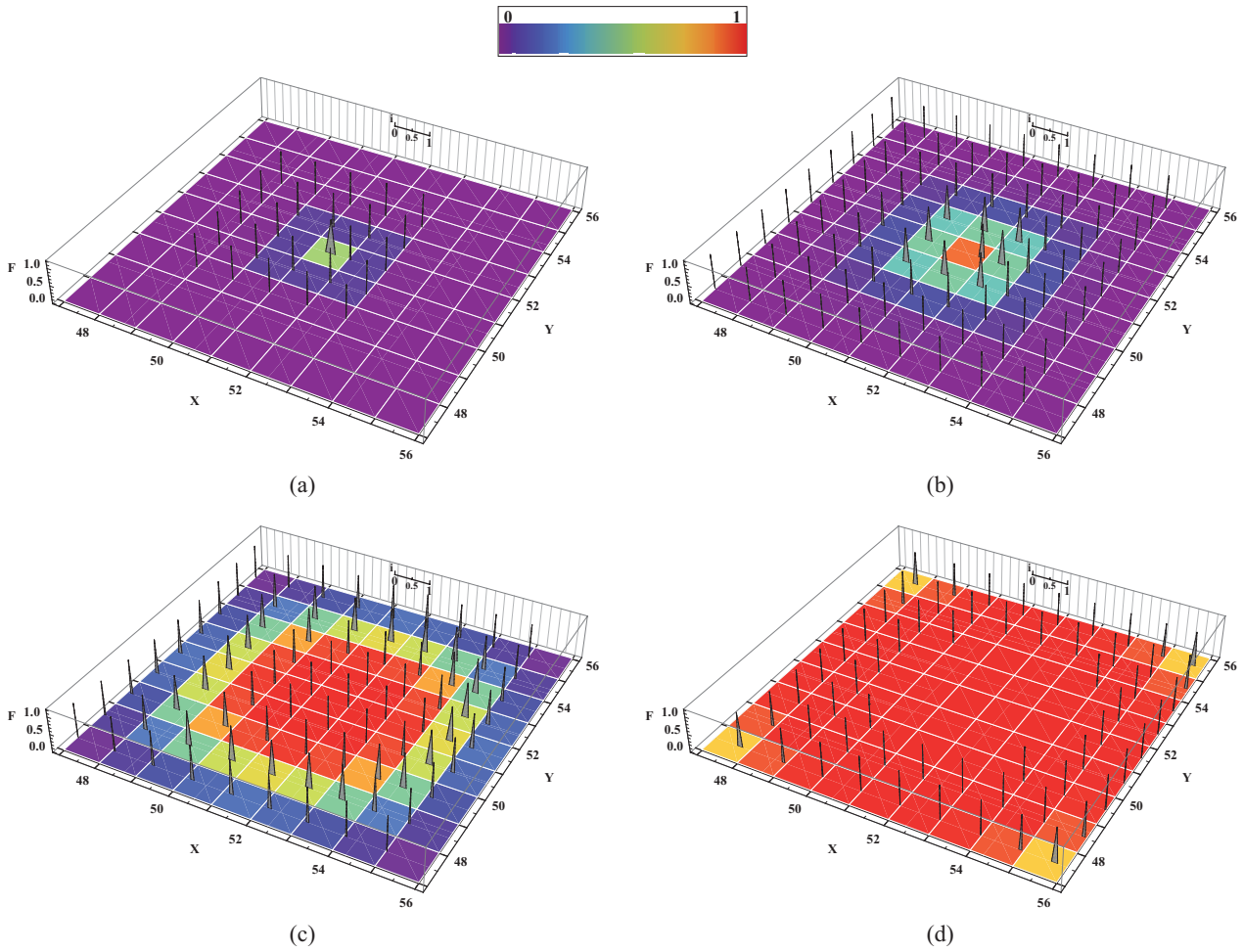

Figure 3: CML state two (a), five (b), ten (c) and fifteen (d) time steps after an outbreak was recorded in the center polygon.

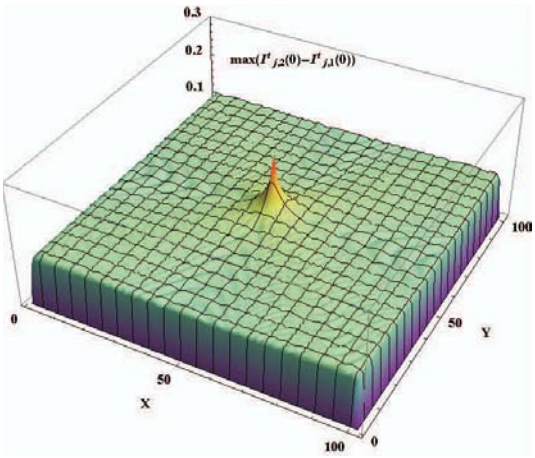

Figure 4: Maximum $[I_c^t]^0$ appeared during the first 125 time steps after an outbreak was recorded in the center polygon of the grid.

the degree of imprecision, expressed as the maximum width of I_j^t's support for all t, decreased asymptotically to 0.1 as d_{cj} increased (Fig. 4).

Also the situation of simultaneous epidemic outbreaks at different locations was studied more closely. For this setup, it can be expected that the imprecision linked to the outbreak data in each of the initially infected polygons might 'interact' when the epidemic waves meet. This was confirmed by the small roughnesses between the two peaks in Fig. 5 showing the maximum width of I_j^t's support during the first 50 time steps after an epidemic was initiated in two polygons which are at distance 14 from one another. Similar to the above-described situation, I_j^t tended to a crisp number as $t \to \infty$ and the CML evolved towards its fixed point.

5 Uncertain epidemic properties

In this section we again consider the model given by (3) with fuzzy initial conditions (10), but in addition we assume that ν_0 was not known accurately and could be described as a triangular fuzzy interval $\nu_0 = (0.2, 0.35, 0.5)$. Comparing Figs. 6 and 3 one clearly sees that I_j^t's support was wider when both the initial condition and ν_0 were only imprecisely known. As the wavefront propagated, the maximum width of the support spanned the entire unit interval in polygons further from P_c due to the successive non-interactive multiplication of ν_0 and $I_{P_i}^t$. Yet, I_j^t tended to a crisp number as $t \to \infty$ since the CML evolved to its fixed point.

6 Conclusions

In this paper it was shown that imprecise information, described using a fuzzy set approach, can be used easily within a spatially explicit model, based upon the coupled-map lattice

ISBN: 978-989-95079-6-8

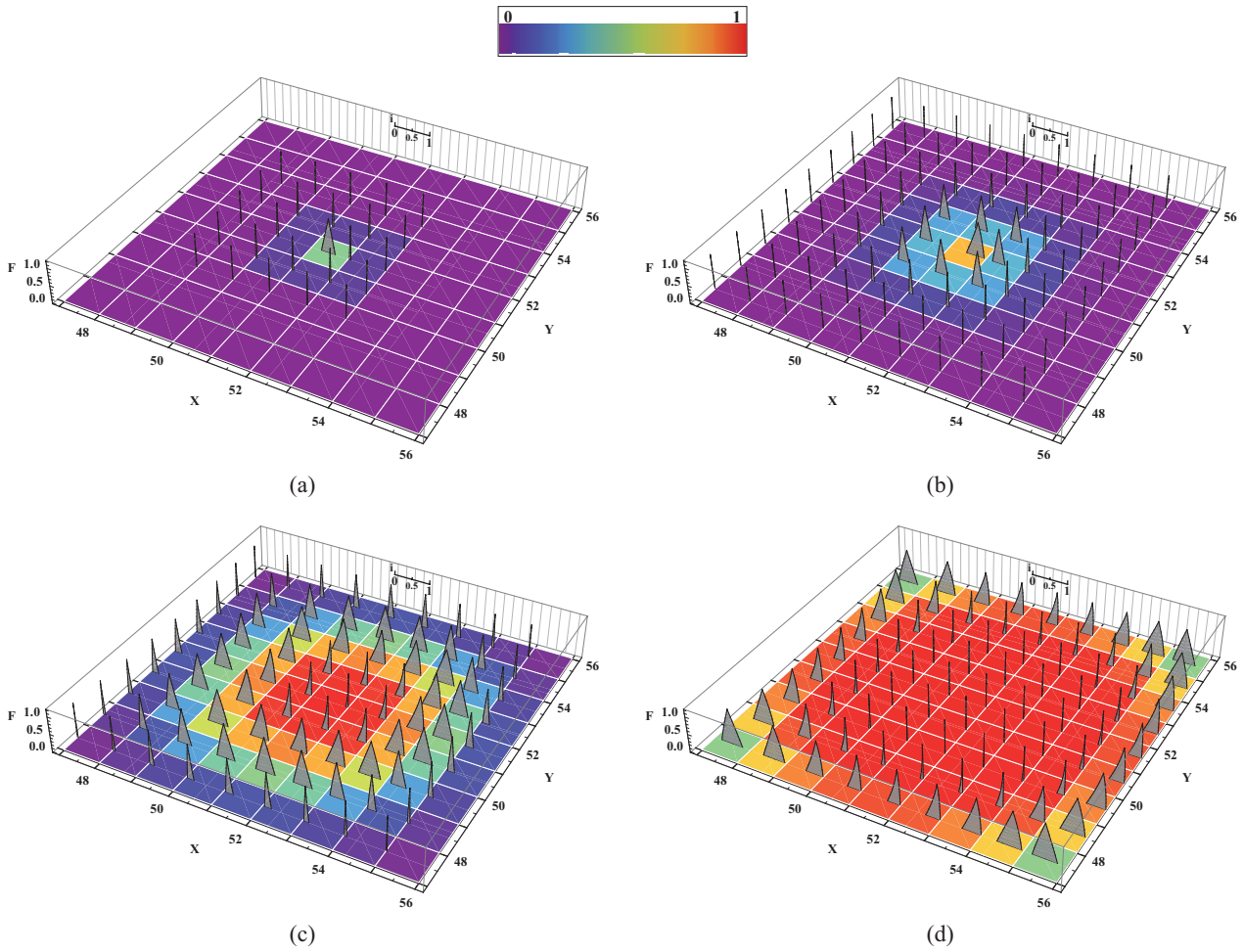

Figure 6: CML state two (a), five (b), ten (c) and fifteen (d) time steps after an outbreak was recorded in the center polygon.

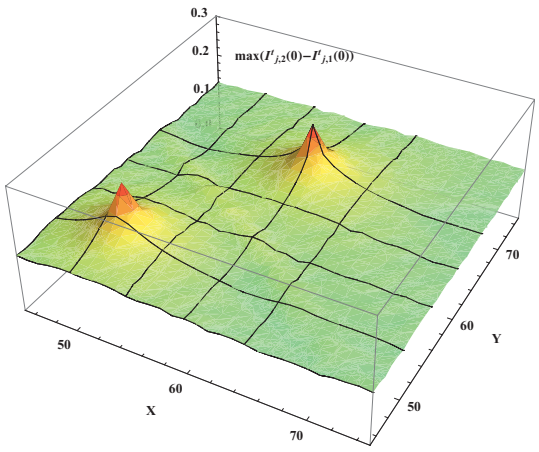

Figure 5: Maximum $[I_c^t]^0$ appeared during the first 125 time steps after an outbreak was recorded in two polygons, which are at distance 14 from one another.

paradigm. The presented modelling framework is perfectly suited to cope with the growing importance and availability of spatio-temporal data. Further work on this topic will consist of extending the presented model to cover also recovered individuals.

References

[1] J.D. Murray. *Mathematical Biology: I. An Introduction*. Springer, Berlin, Germany, second edition, 1993.

[2] J.D. Murray. *Mathematical Biology: II. Spatial Models and Biomedical Applications*. Springer, Berlin, Germany, third edition, 2007.

[3] M. Oberguggenberger and S. Pittschmann. Differential equations with fuzzy parameters. *Mathematical and Computer Modelling of Dynamical Systems*, 5:181–202, 1999.

[4] V. Lakshmikantham and R.N. Mohapatra. Theory of fuzzy differential equations and inclusions. In R.P. Agarwal and D. O'Regan, editors, *Series in Mathematical Analysis and Applications*, volume 6. Taylor & Francis, New York, United States, 2003.

[5] M. Guo and R. Li. Impulsive functional differential inclusions and fuzzy populations models. *Fuzzy Sets and Systems*, 138:601–615, 2003.

[6] J.J. Buckley and T. Feuring. Fuzzy differential equations. *Fuzzy Sets and Systems*, 110:43–54, 2000.

ISBN: 978-989-95079-6-8

[7] Y. Chalco-Cano and H. Román-Flores. On new solutions of fuzzy differential equations. *Chaos, Solitons and Fractals*, 38:112–119, 2008.

[8] D. Vorobiev and S. Seikkala. Towards the theory of fuzzy differential equations. *Fuzzy Sets and Systems*, 125:231–237, 2002.

[9] J.M. Baetens and B. De Baets. A generalized coupled-map lattice to model biological phenomena. *Mathematical Biology*, 2009. Submitted.

[10] S. Wolfram. Statistical mechanics of cellular automata. *Reviews of Modern Physics*, 55:601–644, 1983.

[11] S. Wolfram, editor. *A New Kind of Science*. Wolfram Media Inc., Champaign, United States, 2002.

[12] K. Kaneko, editor. *Theory and Applications of Coupled Map Lattices*. John Wiley & Sons Ltd., Chichester, United Kingdom, 1193.

[13] W.G. Wee and K.S. Fu. A formulation of fuzzy automata and its application as a model of learning systems. *IEEE Transactions on Systems Science and Cybernetics*, 5:215–223, 1969.

[14] M. Doostfatemeh and S.C. Kremer. New directions in fuzzy automata. *International Journal of Approximate Reasoning*, 38:175–214, 2005.

[15] J.N. Mordeson and D.S. Malik. *Fuzzy automata and languages, theory and applications*. Chapman and Hall/CRC, Boca Raton, United States, 2002.

[16] G. Cattaneo, P. Flocchini, C. Quaranta Vogliotti, and N. Santoro. Cellular automata in fuzzy backgrounds. *Physica D*, 105:105–120, 1997.

[17] P. Flocchini, F. Geurts, and N. Santoro. CA-like error propagation in fuzzy CA. *Parallel Computing*, 23:1673–1682, 1997.

[18] D. Dunne and A. Mingarelli. On the dynamics of some exceptional fuzzy cellular automata. In *7th International Conference on Cellular Automata for Research and Industry, ACRI 2006*, pages 78–87, Perpignan, France, September 2006.

[19] S. Assilian. *Artificial Intelligence in the Control of Real Dynamical Systems*. PhD thesis, London University.

[20] E.H. Mamdani. Application of fuzzy algorithms for control of simple dynamic plant. *Proceedings of the IEEE*, 121:1585–1588, 1974.

[21] T. Takagi and M. Sugeno. Fuzzy identification of systems and its applications to modeling and control. *IEEE Transactions on Systems, Man and Cybernetics*, 15:116–131, 1985.

[22] C. Bone, S. Dragicevic, and A. Roberts. A fuzzy-constrained cellular automata model of forest insect manifestations. *Ecological Modelling*, 192:107–125, 2006.

[23] F. Wu. Simulating urban encroachment on rural land with fuzzy-logic-controlled cellular automata in a geographical information system. *Journal of Environmental Management*, 5:293–308, 1998.

[24] M. da Silva Peixoto, L. Carvalho de Barros, and R. Carlos Bassanezi. A model of cellular automata for the spatial and temporal analysis of citris sudden death with the fuzzy parameter. *Ecological Modelling*, 214:45–52, 2008.

[25] M. Mraz, N. Zimic, and J. Virant. Intelligent bush fire spread prediction using fuzzy cellular automata. *Journal of Intelligent and Fuzzy Systems*, 7:203–207, 1999.

[26] Q. Chen and A.E. Mynett. Modelling algal bloom in the Dutch coastal waters by integrated numerical and fuzzy cellular automata approaches. *Ecological Modelling*, 199:73–81, 2006.

[27] L.A. Mentelas, P. Prastacos, and T. Hatzichristos. Modeling urban growth using fuzzy cellular automata. In *Proceedings of the 11th AIGLE Conference (CD-ROM)*, Girona, Spain, 2008.

[28] S. Hoya White, A. Martín del Rey, and G.Rodríguez Sanchez. Modeling epidemics using cellular automata. *Applied Mathematics and Computation*, 186:193–202, 2007.

[29] J. Milne and S C. Fu. Epidemic modelling using cellular automata. In *Proceedings of the 1st Australian Conference on Artificial Life (ACAL'03)*, pages 43–57, Canberra, December 2003.

[30] R.J. Doran and S.W. Laffan. Simulating the spatial dynamics of foot and mouth disease outbreaks in feral pigs and livestock in Queensland, Australia, using a susceptible-infected-recovered cellular automata model. *Preventive Veterinary Medicine*, 70:133–152, 2005.

[31] A.K. Dewdney. Sharks and fish wage an ecological war on the toroidal planet. *Scientific American*, pages 14–22, December 1984.

[32] H. Baltzer, P.W. Braun, and W. Köhler. Cellular automata models for vegetation dynamics. *Ecological Modelling*, 107:113–125, 1998.

[33] A. Qi, X. Zheng, C. Du, and B. An. A cellular automaton model of cancerous growth. *Journal of Theoretical Biology*, 161:1–12, 1993.

[34] D.G. Mallet and L.G. De Pillis. A cellular automata model of tumor-immune system interactions. *Journal of Theoretical Biology*, 239:334–350, 2006.

[35] L. Preziosi. *Cancer Modelling and Simulation*. Chapman & Hall, Boca Raton, United States, 2003.

[36] C. Picioreanu, M.C.M. van Loosdrecht, and J.J. Heijnen. Mathematical modeling of biofilm structure with a hybrid differential-discrete cellular automaton approach. *Biotechnology and Bioengineering*, 58:101–116, 1998.

[37] G. Pizarro, D. Griffeath, and D.R. Noguera. Quantitative cellular automaton model for biofilms. *Journal of Environmental Engineering*, 127:782–789, 2001.

[38] L.B. Kier, P.G. Seybold, and C. Cheng. *Modelling Chemical Systems using Cellular Automata*. Springer, Dordrecht, The Netherlands, 2005.

[39] J.L. Schiff. *Cellular Automata: A Discrete View of the World*. John Wiley & Sons Ltd., Chichester, United Kingdom, 2008.

[40] L. Beale, J.J. Abellan, S. Hodgson, and L. Jarup. Methodologic issues and approaches to spatial epidemiology. *Environmental Health Perspectives*, 116:1105–1110, 2008.

[41] D. Dubois and H. Prade. *Possibility Theory: an Approach to Computerized Processing of Uncertainty*. Plenum Press, New York, United States, 1988.

[42] R. Fullér and P. Majlender. On interactive fuzzy numbers. *Fuzzy Sets and Systems*, 143:355–369, 2004.

[43] P. Majlender. *A Normative Approach to Possibility Theory and Soft Decision Support*. PhD thesis, Åbo Akademi University, Finland, 2004.

[44] C. Carlsson, R. Fullér, and P. Majlender. On possibilistic correlation. *Fuzzy Sets and Systems*, 155:425–445, 2005.

ISBN: 978-989-95079-6-8